Identification of Functional Regions on the Tail of *Acanthamoeba* Myosin-II Using Recombinant Fusion Proteins. II. Assembly Properties of Tails with NH_2- and COOH-Terminal Deletions

John H. Sinard, David L. Rimm, and Thomas D. Pollard

The Department of Cell Biology and Anatomy, The Johns Hopkins University School of Medicine, Baltimore, Maryland 21205

Abstract. We used purified fusion proteins containing parts of the *Acanthamoeba* myosin-II tail to localize those regions of the tail responsible for each of the three steps in the successive dimerization mechanism (Sinard, J. H., W. F. Stafford, and T. D. Pollard. 1989. *J. Cell Biol.* 107:1537–1547) for *Acanthamoeba* myosin-II minifiliment assembly. Fusion proteins containing the terminal ~90% of the myosin-II tail assemble normally, but deletions within the last 100 amino acids of the tail sequence alter or prevent assembly. The first step in minifilament assembly, formation of antiparallel dimers, requires the COOH-terminal ~30 amino acids that are thought to form a nonhelical domain at the end of the coiled-coil. The second step, formation of antiparallel tetramers, requires the last ~40 residues in the coiled-coil. The final step, the association of two antiparallel tetramers to form the completed octameric minifilament, requires residues ~40–70 from the end of the coiled-coil. A region of the tail near the junction with the heads is important for tight packing of the tails in the minifilaments. Divalent cations induce the lateral aggregation of minifilaments formed from native myosin-II or fusion proteins containing a nonmyosin "head," but under the same conditions fusion proteins composed essentially only of myosin tail sequences with very little nonmyosin sequences form paracrystals. The region of the tail necessary for this paracrystal formation lies NH_2-terminal to amino acid residue 1,468 in the native myosin-II sequence.

POLYMERIZATION of myosin into filamentous structures is a multistep process, and as such it is unlikely that a single region of the myosin tail is responsible for all aspects of the assembly process. Myosin assembly properties can be grossly grouped into at least three different classes. First, minifilaments are small bipolar assemblies of myosin containing from 8 to 16 molecules each and can be made with myosin from skeletal muscle (Reisler et al., 1980), smooth muscle (Trybus and Lowey, 1987), *Acanthamoeba* (Pollard, 1982; Sinard et al., 1989), and probably all other myosins as well. Minifilaments are short enough that each molecule overlaps in an antiparallel fashion with at least one other molecule in the minifilament. Second, elongation involves the addition of myosin molecules to an existing antiparallel structure such that the filament length increases, and involves only parallel interactions between the incoming molecules and the molecules already in the filament. Vertebrate skeletal muscle myosin filaments elongate by the addition of parallel dimers (for review, see Davis, 1988). Finally, paracrystal formation has been long recognized as a property of the tail portion of myosin-II molecules. Paracrystals are generally much larger than myosin filaments and have never been shown to be antiparallel structures, but the interactions between the myosin tails may be similar to those in filaments since both have the same axial repeat of 14.5 nm (Cohen et al., 1970; Huxley and Brown, 1967).

In an effort to determine some general principles about myosin assembly, we have analyzed the polymerization of a simple model system, the formation of *Acanthamoeba* myosin-II minifilaments. Myosin-II is the larger of the two classes of myosins found in this soil ameba. It has two heads and a tail 87 nm long (Pollard et al., 1978). Myosin-II is monomeric in high ionic strength buffers (>250 mM KCl), but polymerizes into bipolar minifilaments (Pollard, 1982; Sinard and Pollard, 1989) consisting of eight myosin molecules (Sinard et al., 1989) in low ionic strength buffers. Minifilaments form by three successive dimerization steps (Fig. 1; Sinard et al., 1989), each involving a different type of intermolecular interaction and therefore likely to be mediated by a discrete region of the myosin-II tail. Kinetic analysis of minifilament assembly has allowed a rough determination of the dissociation constant for each step, showing that all are highly favored in low ionic strength buffers, with dissociation equilibrium constants $<5 \times 10^{-11}$, 7×10^{-11}, and 2×10^{-8} M, respectively (Sinard and Pollard, 1990). Minifilaments do not elongate, but divalent cations or acidic

J. H. Sinard's and D. L. Rimm's present address is Department of Pathology, Yale University Medical School, New Haven, CT 06510.

pH can induce the lateral aggregation of minifilaments into "thick filaments" (Pollard, 1982; Sinard and Pollard, 1989). This lateral aggregation is likely to involve interactions similar to those in myosin paracrystals.

Here we use a molecular biological approach to define the parts of the myosin-II tail that are required for these assembly reactions. A number of cDNA fragments for the *Acanthamoeba* myosin-II heavy chain, as well as a full-length cDNA, have been isolated and many of these have been expressed in *Escherichia coli* using the pATH-11 and pRX expression vectors (Rimm et al., 1989, 1990; Rimm and Pollard, 1989). In a previous paper, we used expressed myosin-II fragments to identify the amino acid residues that form the binding site for several monoclonal antibodies and the physical head–tail junction (Rimm et al., 1989). Here, we describe the purification and characterization of multiple bacterially expressed fusion proteins containing regions of the myosin-II tail. The myosin-II portions of these fusion proteins fold into an alpha-helical coiled-coil structure and the purified proteins are functional in in vitro assembly assays. Characterization of these proteins, in combination with information in the literature, allowed us to localize the regions of the tail involved in each of the four assembly reactions and to identify a novel region in the proximal part of the tail that may stabilize interactions between parallel molecules with a 15-nm stagger.

Materials and Methods

Clones and Expression Systems

The isolation of cDNA clones and expression of fusion proteins in both the pATH-11 and the pRX expression vectors is described elsewhere (Rimm et al., 1989, 1990).

Purification of Expressed Fusion Proteins from E. coli

Overnight cultures (50 ml) were inoculated into 500 ml of M9+CA medium (Maniatis et al., 1982), grown for 3–4 h and then induced with 10 μg/ml indolyl acrylic acid for 4–5 h. Bacteria were harvested by centrifugation and washed in 10 mM Tris pH 8.0. The cell pellet was then resuspended in 70 ml of 10 mM Tris pH 8.0, 8% sucrose, 50 mM EDTA, 0.5% Triton X-100, 2 mg/ml lysozyme (Sigma Chemical Co., St. Louis, MO) with 10 μg/ml each of chymostatin, leupeptin, antipain, and pepstatin-A (Sigma Chemical Co.), incubated on ice for 20–30 min, and then sonicated with ~6 × 30-s bursts with a Sonifier Cell disrupter 200 (Branson Sonic Power Co., Danbury, CT). The sonicate was then centrifuged for 10 min at 10,000 rpm in a JA-20 rotor (Beckman Instruments, Inc., Palo Alto, CA), and the supernatant used for subsequent purification. All of the fusion proteins were purified by the same procedure consisting of four steps: ammonium sulfate fractionation, gel filtration, anion exchange chromatography, and hydroxylapatite chromatography, all performed at 4°C. At each step, samples of column fractions were electrophoresed on an SDS-polyacrylamide gel and the fractions of interest identified initially by blotting onto nitrocellulose and reacting with pooled monoclonal antibodies to myosin-II, and later simply by Coomassie blue staining. A 1.0–2.5-M ammonium sulfate cut was used. In all cases, the 1.0-M cut formed a precipitate of lower density than the soluble fraction and was therefore centrifuged to the top of the tube. The 2.5-M ammonium sulfate pellet was resolubilized in a minimum volume of A-15m buffer and loaded onto a 2.5 × 45 cm column of BioGel A-15m (Bio-Rad Laboratories, Rockville Center, NY) equilibrated with 10 mM imidazole, pH 7.5, 600 mM KCl, 5% sucrose, 1 mM dithiothreitol, 0.02% sodium azide, 0.1 mM benzamidine, 1 mM PMSF. The fusion proteins eluted in the leading edge of the protein peak. Fractions containing the fusion protein were pooled and dialyzed against two changes of DEAE buffer (10 mM imidazole, pH 7.5, 20 mM KCl, 1 mM dithiothreitol, 0.02% sodium azide). This pool was loaded onto a 1.5 × 20-cm column of DE-52 (Whatman, Maidstone, England) and eluted with a 100-ml linear gradient of 20–600 mM KCl. At this point, many of the fusion proteins were >90% pure, and the desired fractions were pooled and concentrated. If greater purification was needed, the pool was loaded directly onto a 1.5 × 15-cm column of hydroxylapatite (Bio-Rad Laboratories, Richmond, CA) and eluted with a 90 ml 0–1-M concave gradient of potassium phosphate, pH 7.5. Fractions containing the purified fusion protein were concentrated against solid sucrose and then dialyzed into storage buffer (10 mM imidazole, pH 7.5, 10% sucrose, 1 mM dithiothreitol, 0.02% sodium azide).

Electron Microscopy

Samples for electron microscopy, typically at ~60 μg/ml protein, were sprayed on to mica and rotary shadowed (Sinard et al., 1989). Micrographs were recorded at 25,000–50,000× in a Zeiss EM10A electron microscope. Dimensions of molecules were measured on 8 × 10 prints using an eyepiece micrometer or on images projected with an enlarger using a ruler. Magnifications were calibrated using negatively stained tropomyosin paracrystals.

Light Scattering Assay

90° light scattering at 365 nm of 1 ml solutions were measured in a fluorescence spectrophotometer (model 650-105; Perkin-Elmer Corp., Norwalk, CT) zeroed on an appropriate buffer blank. The details of this assay are described by Sinard and Pollard (1989). To correct for differences in the light scattering intensity from molecules of different sizes and slightly different concentrations, the light scattering values were normalized to the scattering intensity at 300 mM KCl where all of the molecules are monomeric.

Other Materials

Myosin-II was purified as described (Sinard and Pollard, 1989). M2.46 is a monoclonal antibody to myosin-II that binds to the tail between amino acid residues 1,048 and 1,102 (Rimm et al., 1989). Protein concentrations were determined by a variety of methods, all using myosin-II as a standard, including the Bradford protein assay (Bio-Rad Laboratories), absorbance at 280 nm, and light scattering intensity of monomers. The fusion proteins expressed in the pRX vector consisted of essentially only myosin tail. They had very low absorbance at 280 nm, consistent with the presence of no tryptophans and only two tyrosines (Hammer et al., 1987), and did not react with the Bio-Rad Laboratories reagent. For these proteins, concentrations were estimated by precipitation with tannic acid and reading the absorbance at 490 nm relative to myosin-II standards (Mejbaum-Katzenellenbogen and Dobryszycka, 1959).

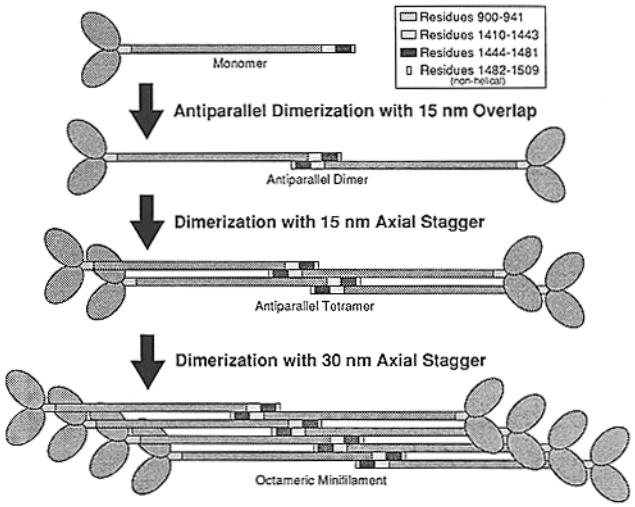

Figure 1. The assembly mechanism for *Acanthamoeba* myosin-II minifilaments. Regions of the tail especially important for assembly (see Fig. 13) are highlighted. It should be noted that the structures of the tetramer and minifilament are two-dimensional representations of a three-dimensional structure and are not meant to represent the actual packing arrangement of the tails.

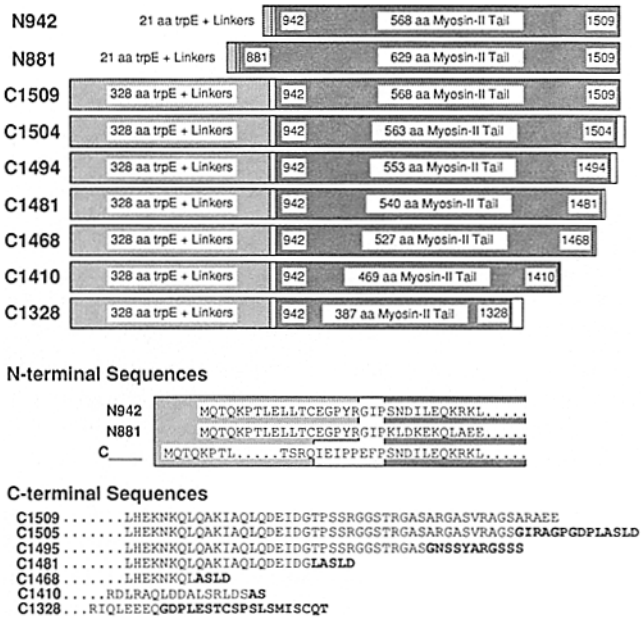

Figure 2. A schematic representation of the sources of the coding sequences for the fusion proteins. The dark shaded area is derived from myosin-II, the light shaded area is derived from the trpE gene product, and the unshaded area represents nonmyosin residues derived from the linker or vector sequences. Each region is drawn to scale. The amino acid sequences of the ends of the clones are shown using the single letter code. COOH-terminal nonmyosin-II sequences are in boldface.

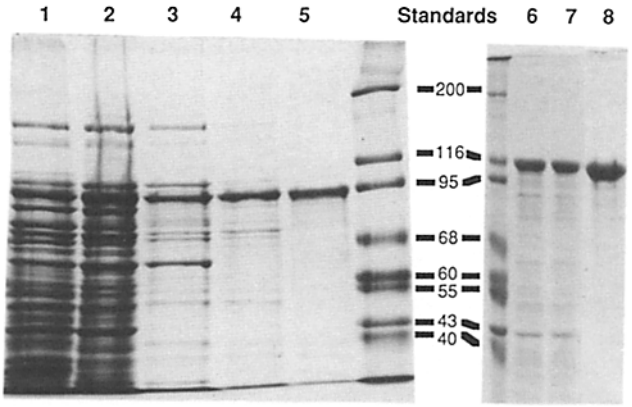

Figure 3. Coomassie blue-stained polyacrylamide gel of fractions obtained from each step in the purification of C1,328 (lanes *1–5*) and C1,468 (lanes *6–8*). Lanes are (*1* and *6*) bacterial extract after low speed spin, (*2* and *7*) resuspended 1.0–2.5 M ammonium sulfate cut, (*3* and *8*) A-15m gel filtration column pool, (*4*) DE-52 column pool, and (*5*) hydroxylapatite column pool. Mobilities of molecular mass standards are given in kilodaltons.

Results

Fusion Protein Constructs

Clones expressed in pRX (Rimm and Pollard, 1989) contain 21 nonmyosin-II amino acid residues at the NH_2 terminus (Fig. 2) and are named for the residue at the NH_2 terminus

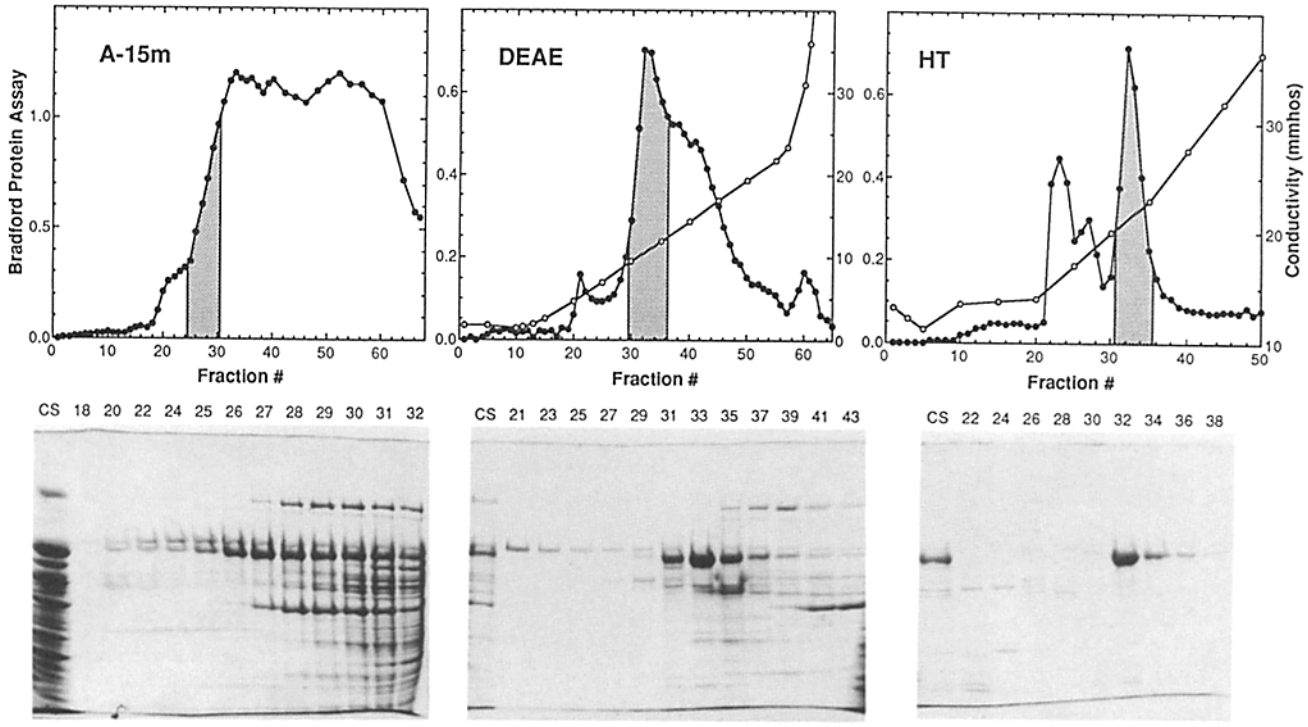

Figure 4. Column profiles from the chromatography steps used to purify C1,328. The shaded areas represent the fractions pooled for further purification. (●) Relative protein concentrations, in arbitrary units. (○) Conductivity in mmhos. For each gel, *CS* represents the column sample, and numbers refer to column fractions. *A-15m*, Biogel A-15m column. *DEAE*, Whatman DE-52 column. *HT*, hydroxylapatite column.

of the myosin-II sequence, preceded by the prefix "N." These pRX fusion proteins end at residue 1,509, the native COOH terminus of myosin-II.

Clones expressed in pATH-11 begin with 328 amino acids of the bacterial trpE gene product, followed by eight residues from the polylinker sequences and a variable number of myoxin-II tail residues beginning with serine-942 and proceeding toward the COOH terminus (Fig. 2). These fusion proteins are named with the prefix "C" followed by the number of the COOH-terminal-most myosin-II amino acid residue contained within the fusion protein. Thus, C1,509 extends to the native COOH terminus of myosin-II and uses the native stop codon. Other deletions contain 2–19 non-myosin-II residues at the very COOH terminus before a stop codon is reached (Fig. 2).

Purification of Fusion Proteins

All of the fusion proteins were purified by essentially the same procedure. After ammonium sulfate fractionation and gel filtration to remove the DNA, RNA, and most of the bacterial proteins, the partially purified fusion proteins were chromatographed on DEAE and then, if <90% pure, on hydroxylapatite. In general, larger clones such as C1,468 (Fig. 3) were easier to purify because they separated better from contaminants on gel filtration.

The purification of C1,328 is illustrated (Figs. 3 and 4) as an example of a fusion protein that was difficult to purify. High-speed extracts of bacteria containing this fusion protein have a prominent 95-kD band (Fig. 3, lane *1*). This band cross-reacts on blots with antibodies to the tail portion of myosin-II, and is not present in extracts of bacteria lacking the fusion protein gene (data not shown). The 1.0–2.5-M ammonium sulfate precipitation (Fig. 3, lane *2*) removes much of the contaminating nucleic acid and concentrates the sample. The fusion protein elutes at the leading edge of the protein peak on the gel filtration column (Fig. 4), as expected for a highly asymmetrical molecule, and elutes as the major peak on the DEAE column. Minor contaminants were further reduced by hydroxylapatite chromatography. Densitometry scan of a Coomassie blue–stained SDS-PAGE sample of the pool from the final column (Fig. 3, lane *5*) shows that the fusion protein was ~90% pure.

The yield of fusion protein varied from 2–20 mg per 500 ml culture due to variable levels of expression. Those expressed in high levels were >90% pure after the DEAE chromatography step (e.g., C1,468; Fig. 3, lanes *6–8*) and therefore were not chromatographed on hydroxylapatite.

Myosin Tail Portions of the Fusion Proteins Form Native Alpha-Helical Coiled-Coils

Proteins expressed in pATH-11, which contain 336 amino acids of the bacterial trpE protein at their NH_2 terminus, look like lollipops with a tail extending from a single large head (Fig. 5, *c* and *d*). The tail is the same width but shorter than that of native myosin-II, and the single head is larger than a native myosin-II head (compare with Fig. 5 *a*). We believe that these monomers consist of two identical polypeptide chains in which the myosin-II tail domains fold into an alpha helical coiled-coil forming the tail, with the two NH_2-terminal trpE chains folding together into a single globular structure comprising the large head. Occasionally,

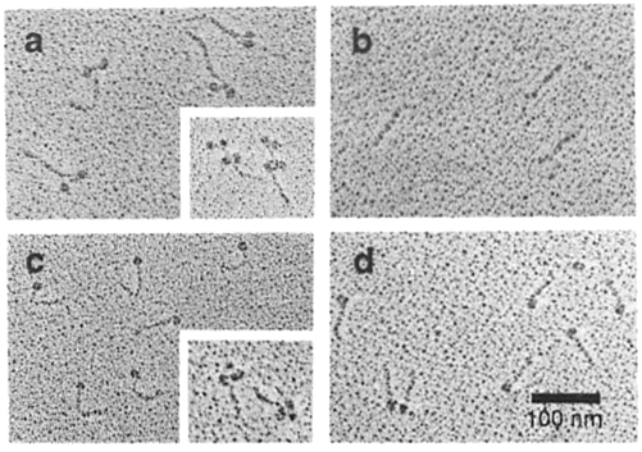

Figure 5. Electron micrographs of rotary-shadowed myosin and recombinant myosin molecules. (*a*) Myosin-II, (*b*) N942, (*c*) C1,509, (*d*) C1,328. Insets in *a* and *c* show the respective molecules decorated with monoclonal antibody M2.46, which binds to the tail between amino acid residues 1048 and 1102 (Rimm et al., 1989).

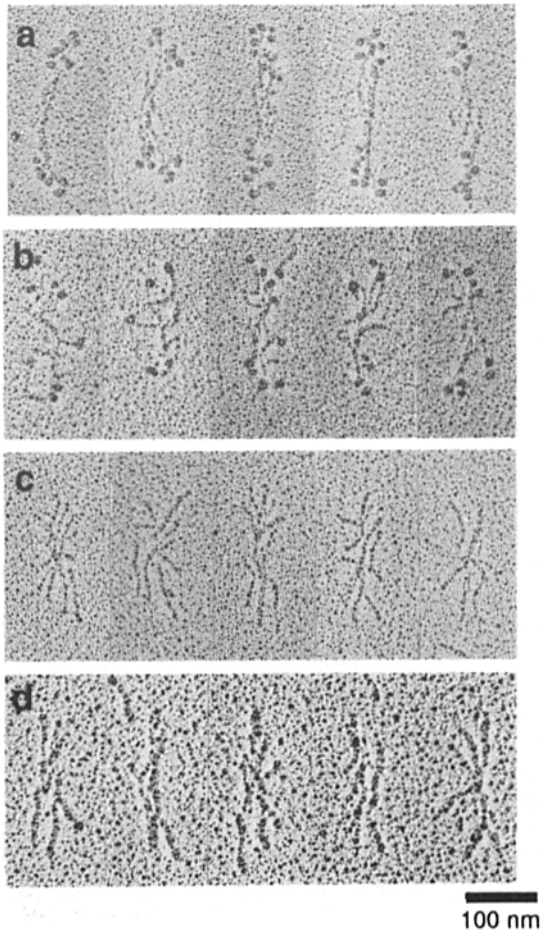

Figure 6. Electron micrographs of rotary-shadowed myosin and fusion protein minifiliaments formed in low salt (50 mM KCl). (*a*) Myosin-II, (*b*) C1,509, (*c*) N942, (*d*) N881.

the head can be resolved into two smaller structures (data not shown). The presence of two polypeptide chains in each of the molecules is confirmed by the fact that C1509 monomers, like native myosin-II monomers, each bind two molecules of the monoclonal antibody M2.46 (Fig. 5, *a* and *c*, *insets*). The fusion proteins expressed in pRX, on the other hand, appear as simple rods with the same thickness as the myosin-II tail (Fig. 5 *b*). The lack of a marker for the NH_2-terminus of this protein makes it impossible to determine visually the polarity of this molecule.

The tails of fusion proteins lacking the trpE "head" are precisely as long as expected from the number of myosin-II amino acid residues contained within the sequence, assuming a 0.148-nm rise per residue and 27 nonalpha-helical residues at the native COOH-terminus (see Rimm et al., 1989). The tails of N942 and N881 average 79.2 and 87.5 nm long. On the other hand, the tails of all fusion proteins with trpE heads are ~10 nm shorter than the predicted lengths. In particular, the tail of C1,509, which has precisely the same myosin-II residues as N942, is 69.5 nm long, 9.7 nm shorter than the tail of N942. The monoclonal antibody M2.46 binds to these "short tails" the same distance from the tip of the tail as for native myosin-II (Fig. 5, *a* and *c*, *insets*), indicating that the "missing" 10 nm is absent from the NH_2 terminus of the tail, undoubtedly either obscured by the large trpE head or prevented from folding properly because of the presence of the trpE domains. Either way, the first amino acid residue of the native myosin-II tail available for polymerizing interactions in the fusion proteins containing a trpE head is approximately residue 1010.

Fusion Proteins with Full-length Tails Assemble into Minifilaments by the Same Mechanism as Native Myosin-II

In 50 mM KCl, all of the fusion proteins that extend to the COOH terminus of native myosin-II formed small bipolar structures very similar to native myosin-II minifilaments. Native filaments are 230 nm long and contain four pairs of heads in each half filament, staggered axially by 15 nm (Fig. 6 *a*; also Sinard et al., 1989). The location of the trpE heads of the C1,509 molecules at either end of the minifilament formed by this fusion protein (Fig. 6 *b*) indicate that these molecules assemble with the same polarity as native myosin-II. In general, four heads can be seen on each half filament, indicating that, like native myosin-II, C1,509 forms minifilaments consisting of eight monomers each. Although difficult to judge because of the looseness of the filaments, the stagger between the monomers in favorable filaments is ~15 nm. Minifilaments formed by N942 and N881 (Fig. 6, *c* and *d*) also contain eight molecules each, although the polarity of the molecules cannot be determined directly. In each of these cases, essentially all of the fusion protein molecules formed these minifilaments, and very few assembly intermediates were seen.

At intermediate salt concentrations, C1,509 formed both antiparallel dimers (Fig. 7, *top row*) and antiparallel tetramers (Fig. 7, *bottom row*) as assembly intermediates just like native myosin-II (Sinard et al., 1989). These intermediates have a mean dimer head-to-head spacing of 123.0 nm, a total dimer length of 156.8 nm, and a total tetramer length of 171.9 nm. Since C1,509 monomers have tails 69.5 nm long, the above measurements indicate that dimers form with a tail

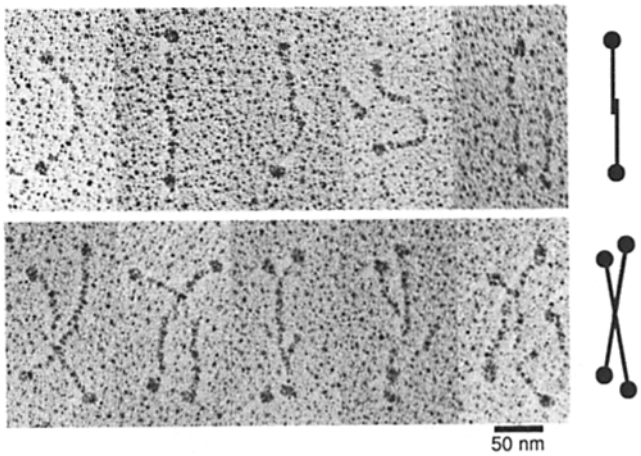

Figure 7. Electron micrograph of C1,509 minifiliment assembly intermediates, prepared by rotary shadowing. (*Top row*) Antiparallel dimers. (*Bottom row*) Tetramers.

overlap of ~16 nm and that tetramers are formed by the lateral association of two antiparallel dimers with a 15-nm stagger, in very close agreement with the 15-nm value for both of these measurements for native myosin-II.

Fusion Proteins Lacking the Proximal (NH_2-Terminal) Part of the Myosin-II Tail from "Loose" Minifilaments

After drying and shadowing the molecules in the C1,509 and N942 minifilaments appeared to be more loosely packed

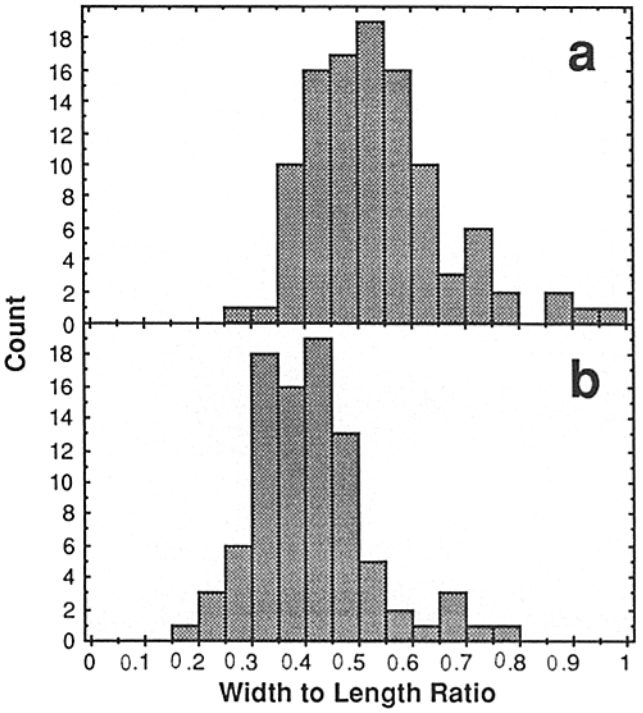

Figure 8. Frequency distributions of the width-to-length ratios of minifiliaments formed from N942 and N881. Measurements are from electron micrographs of rotary-shadowed images. (*a*) N942: $n = 105$, mean = 0.54, SD = 0.13 (*b*) N881: $n = 89$, mean = 0.41, SD 0.11.

than native myosin-II minifilaments (Fig. 6). The C1,509 and N942 molecules were tethered in the bare zone region but separated more freely from each other at both ends of the minifilament than either N881 (Fig. 8) or native myosin-II minifilaments. The difference is statistically significant ($P = 0.0001$ in an unpaired t-test). Negatively stained fusion protein minifilaments do not routinely show this loose association, suggesting that forces during the drying of the samples onto the mica before shadowing are important for revealing the instability of the lateral interactions.

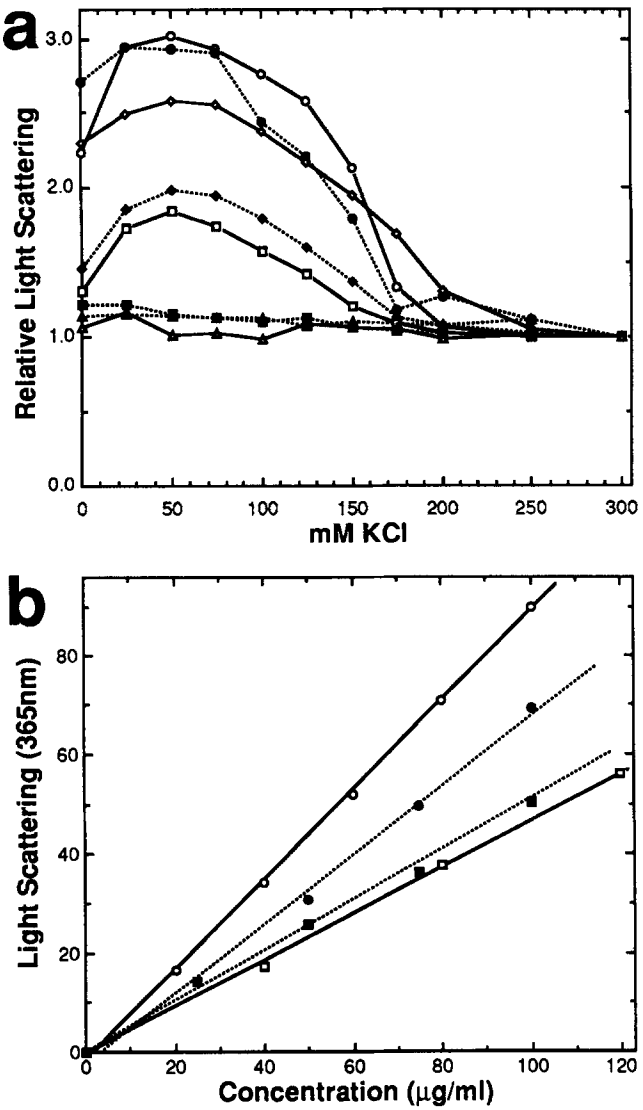

Figure 9. Relative 90° light scattering intensity of myosin-II and fusion proteins. (*a*) Light scattering of ~50 μg/ml fusion protein in 9 mM imidazole, pH 7.0, 1% sucrose as a function of the KCl concentration. The light scattering has been normalized to the scattering intensity at 300 mM KCl. (○) Native myosin-II, (●) C1,509, (◇) C1,504, (◆) C1,494, (□) C1,481, (■) C1,468, (△) C1,410, (▲) C1,328. (*b*) Light scattering intensity under assembly conditions (50 mM KCl) as a function of concentration of fusion protein or myosin-II. (○) Native myosin-II, (●) C1,509, (□) C1,481, (■) N942.

Fusion Proteins Containing COOH-Terminal Deletions (Short Tails) Show Altered Assembly Properties

We used a light scattering assay (Sinard and Pollard, 1989) to quantitate the salt-dependent assembly properties of the fusion proteins. The light scattering of native myosin-II, C1,509 (Fig. 9 *a*) and N942 (not illustrated) shows nearly the same dependence on salt concentration. Above 200 mM KCl, the proteins are monomeric. Between 25 and 100 mM KCl, the light scattering is maximal at about three times the monomer value. Between 100 and 200 mM KCl, the light scattering declines with salt concentration. There is also a slight drop in scattering at salt concentrations below 25 mM KCl. Like native myosin-II, both N942 and C1,509 in 50 mM KCl show a linear dependence of light scattering intensity on protein concentration, and these lines intersect the concentration axis very near the origin, indicating that they all have critical concentrations for assembly <5 μg/ml (Fig. 9 *b*).

To determine which regions of the myosin-II tail are required for minifilament formation, we quantitated the assembly properties of fusion proteins containing known deletions from the COOH terminus. Deletion of the last five amino acids (C1,504), even with the addition of 14 non-myosin-II amino acids from random read into the vector (Fig. 2), had a minimal effect on the light scattering (Fig. 9 *a*). Deletion well into the nonalpha-helical tail piece (C1,494) or removal of the entire tail piece (C1,481) resulted in decreased light scattering at low ionic strength without changing the salt dependence (Fig. 9 *a*). Although reduced, the light scattering of C1,481 depended linearly on the protein concentration, and extrapolated to a low critical concentration for polymerization (Fig. 9 *b*, C1,481). This decreased light scattering was accompanied by an increase in the relative number of monomers and partially assembled polymers, as viewed in the electron microscope. For C1,481, parallel dimers rather than antiparallel dimers were seen as assembly intermediates (Fig. 10). These parallel dimers had subunits staggered axially by ~15 nm. For C1,495, both parallel and antiparallel dimers were observed (data not shown).

C1,468 showed essentially no assembly by light scattering in the absence of Mg (Fig. 9 *a*). Electron microscopy, how-

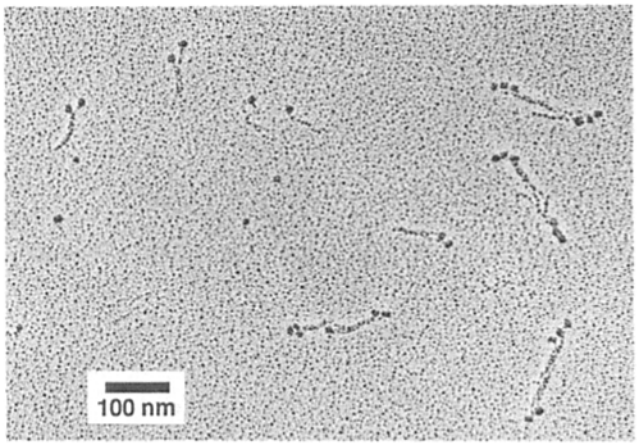

Figure 10. Electron micrograph of a field of C1,481 molecules, rotary shadowed in 25 mM KCl. Note the presence of parallel dimers and the absence of antiparallel dimers.

ever, did reveal the presence of a few fully assembled minifilaments, as well as a few tetramers, antiparallel dimers and parallel dimers, but the large majority of the molecules were monomeric. Larger COOH-terminal deletions resulted in molecules (C1,410, C1,328) for which no evidence of assembly could be demonstrated by any assay. In fact, a field of rotary-shadowed C1,328 molecules under assembly conditions (Fig. 5 *d*) is indistinguishable from a field at 300 mM KCl.

Mg^{++} Induces the Formation of Higher Order Structures

In the presence of millimolar concentrations of divalent cations, both myosin-II and C1,509 minifilaments show a Mg^{++}-dependent increase in light scattering (Fig. 11 *a*), and this correlates with the lateral aggregation of the minifilaments into a heterogeneous population of thick filaments (Fig. 12, *a* and *b*; Pollard, 1982; Sinard and Pollard, 1989). Lateral striations, spaced at 15-nm intervals, are clearly visible at both ends of the thick filaments formed from C1,509 (Fig. 12 *b*). These striations are only occasionally preserved in myosin-II thick filaments (Pollard, 1982).

As with the fusion proteins extending to the native COOH terminus of the myosin-II tail, fusion proteins containing small deletions from the tip of the tail could also be aggregated by divalent cations, and C1,481 showed the same Mg^{++}-dependent increase in light scattering as seen for C1,509 (Fig. 11 *a*). C1,468, which showed significantly decreased assembly properties in the absence of Mg^{++}, could

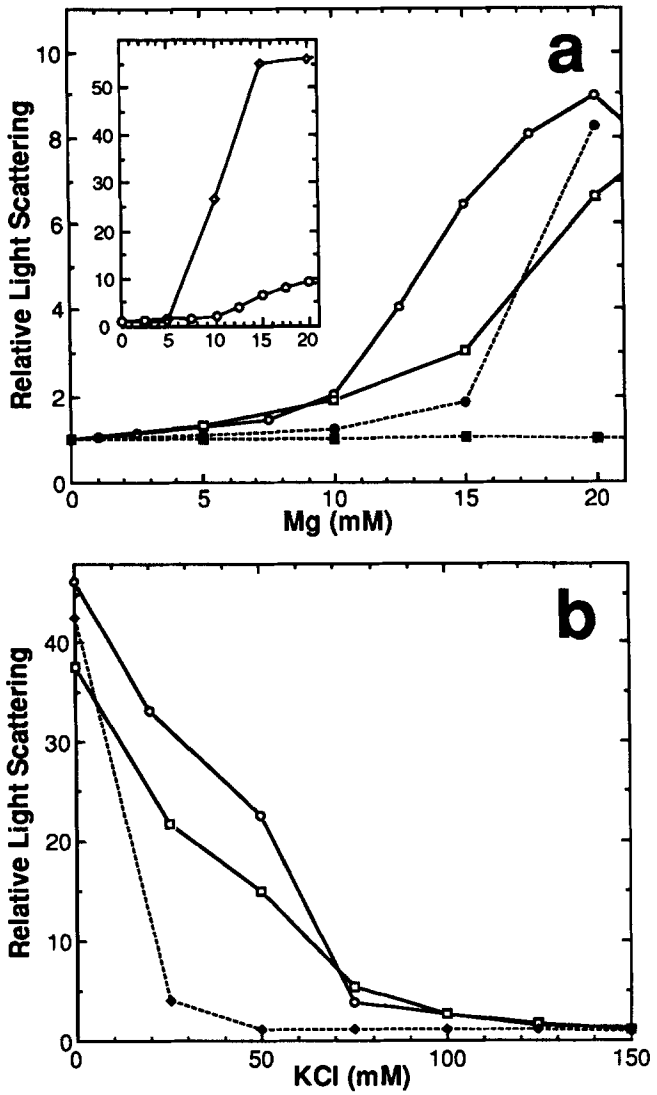

Figure 11. Effect of Mg^{++} on the light scattering intensity of myosin-II and fusion proteins under polymerizing conditions. 90° light scattering at 365 nm was determined in 8 mM imidazole, pH 7.0, ~1% sucrose, and either (*a*) 50 mM KCl with $MgCl_2$ as indicated (normalized to the scattering intensity at 0 mM Mg^{++}), or (*b*) 20 mM $MgCl_2$ with KCl as indicated (normalized to the scattering intensity at 300 mM KCl). The inset in *a* contains an expanded scale. (○) Native myosin-II, (●) C1,509, (□) C1,481, (♦) C1,468, (■) C1,328, and (◇) N942.

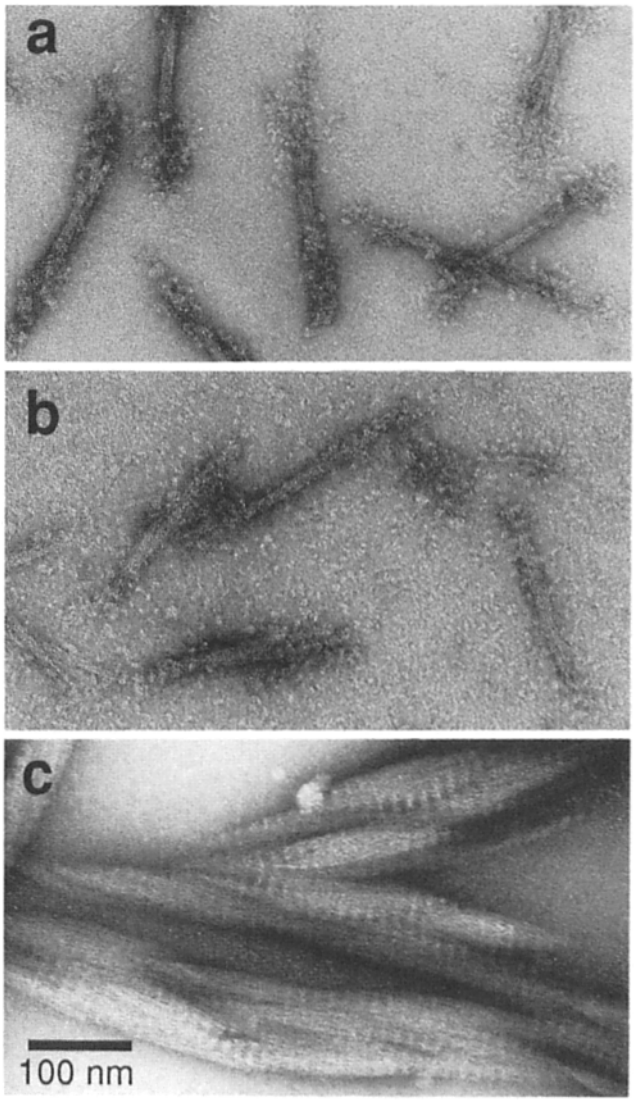

Figure 12. Electron micrographs of negatively stained myosin-II and fusion proteins in the presence of divalent cations: (*a*) native myosin-II, (*b*) C1,509, and (*c*) N942. Conditions: 9 mM imidazole, pH 7.0, 50 mM KCl, 20 mM $MgCl_2$. Myosin-II and C1,509 form thick filaments, but under the same conditions N942 forms paracrystals.

also be induced to form thick filaments with a resulting increase in light scattering by the addition of Mg^{++}, but this effect was seen only at very low KCl concentrations (Fig. 11 *b*). Larger deletions resulted in no assembly, even in the presence of 20 mM $MgCl_2$ (Fig. 11 *a*, C1328).

The fusion protein N942, which lacks the trpE head, shows a much greater increase in light scattering upon addition of Mg^{++} than either C1509 or native myosin-II, forming paracrystals up to several micrometers long (Fig. 12 *c*) that scatter approximately five times as much light as thick filaments (Fig. 11 *a*, *inset*). The repeat distance of these paracrystals measures 14.8 nm. The paracrystals form at slightly lower concentrations of Mg^{++} than are necessary to induce thick filament formation (Fig. 11 *a*, *inset*).

Discussion

The use of bacterially expressed fragments of a protein to investigate the relationship between structure and function has many advantages compared with proteolytic dissection, especially the power to produce and modify any region of the polypeptide chain. Other advantages include the ability to obtain the expressed fragment without the heterogeneities that might be introduced by posttranslational modifications such as phosphorylation. On the other hand, this approach has many limitations and potential pitfalls. Short of x-ray crystallography, it is usually difficult to establish that a fragment of a protein expressed in a fusion protein has folded correctly in the absence of other parts of the polypeptide, posttranslational modifications or the association of other protein subunits.

For the tail of myosin, many of the disadvantages of using bacterially expressed cloned fragments do not exist. The myosin-II tail is formed by an alpha-helical coiled-coil of two polypeptide chains. Since it is essentially a one-dimensional structural, one can be less concerned about the absence of missing regions altering the folding of fragments. Also, the alpha-helical coiled-coil is very stable, increasing both its chances of folding properly in a nonnative environment and its stability in the presence of foreign proteases, and the highly asymmetric nature of the structure aids in its purification.

Fusion Proteins Are Purified with the Myosin-II Tail Sequences Folded into their Native Conformation

We purified fragments of the myosin-II tail without cycles of polymerization and depolymerization to avoid a bias in favor of proteins competent to assemble. We also avoided harsh conditions such as precipitation with organic solvents or heating, which might have subtle adverse effects on the structure and therefore the function of the purified proteins.

The tail of the purified full-length fusion proteins are almost certainly in the native conformation, because they polymerize by the same pathway and to the same extent as native myosin-II. Thus, both the coiled-coil and the COOH-terminal nonhelical domain fold properly in the fusion proteins. The conformation of the truncated fusion proteins is less certain, but by EM they are the length expected for a fully alpha-helical coiled coil. There could be subtle folding defects at the COOH termini of these fusion proteins (especially those with nonmyosin residues), but in the presence of hundreds of helical residues this would be difficult to detect even with circular dichroism measurements.

Small Regions Near the End of the Tail Are Required for Each of the Three Steps in Minifilament Assembly

Although the tail of myosin-II has a uniform structure and pattern of alternating charges (Hammer et al., 1987), the profound effects of small COOH-terminal deletions show that not all parts contribute equally to the assembly of minifilaments. Each of 3 short sequences within the last 100 residues is essential for one of the 3 steps in minifilament formation (Figs. 1 and 13) and the star-shaped octamers formed from tails compromised at their NH_2 termini (Fig. 6) confirm the importance of intermolecular bonds between the ends of the tails. Although the sites identified in Fig. 13 are essential for assembly they are not sufficient, because they must interact with complementary sites, some of which have been identified with monoclonal antibodies (Rimm et al., 1990).

Since minifilament assembly occurs in three discrete steps, it is reasonable to postulate that each step is mediated

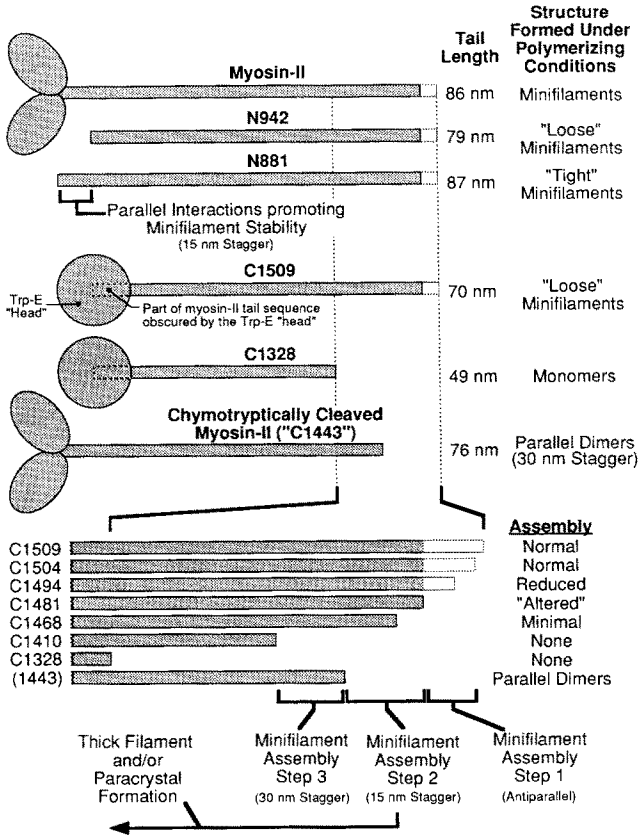

Figure 13. A summary of myosin-II and fusion protein structures. Tail lengths, the structures formed under polymerizing conditions and the regions we suggest are important for the intermolecular interactions mediating various types of assembly reactions, are shown. The unfilled dashed region at the end of the tails represents the nonhelical 27 amino acid long tail piece. The nonmyosin-II sequences at the COOH terminus are not illustrated. Data on chymotryptically cleaved myosin ('C1443') was obtained from Kuznicki et al. (1985).

by unique intermolecular interactions (Fig. 1; Sinard et al., 1989; Sinard and Pollard, 1990). In the following paragraphs we analyze the collective evidence that supports this hypothesis.

Step 1. All lines of evidence indicate that the high affinity ($K_d \leq 5 \times 10^{-11}$ M) formation of antiparallel dimers depends on the association of the nonhelical tail piece (residues 1,481–1,509) with the coiled-coil at a site near residue 1,380. First, at high salt concentrations myosin-II forms some "half-assembled" dimers with the very tip of one tail associated with a second molecule at a point 15 nm from the end of its tail (see Fig. 11, Sinard et al., 1989). Second, stepwise truncation of the tail from 1,509 to 1,468 results in a progressive failure to form antiparallel dimers and assemble minifilaments: C1,495 forms both parallel and antiparallel dimers; C1,481 forms parallel dimers before any antiparallel structures (Fig. 10); and C1,468 forms a few antiparallel dimers (data not shown) but gives no light scattering signal (Fig. 9 *a*). Given the importance of the tail piece in assembly, it is remarkable that phosphorylation of two serines in the tail piece (Coté et al., 1984) has no detectable effect on minifilament assembly (Sinard and Pollard, 1989).

Although the terminal 15 nm of coiled-coil composed of residues 1,380 and 1,480 does not support efficient dimerization, it must contribute some bond energy to the dimer. First, electron microscopy shows a close association between the last 15 nm of the two tails (Sinard et al., 1989). Second, even molecules lacking the entire tail piece form a few antiparallel dimers. Third, monoclonal antibodies binding to three sites between residues 1,399 and 1,467 can partially or completely inhibit dimerization (Rimm et al., 1990).

Step 2. The assembly properties of three fragments revealed a short sequence essential for step 2. C1,481 is competent for both steps 2 and 3, but C1,410 can accomplish neither. A proteolytic fragment of myosin-II essentially equivalent to "C1,443" (Kuznicki et al., 1985; Hammer et al., 1987; Wijmenga et al., 1987) forms parallel dimers with a 30-nm stagger (step 3) but not 15-nm staggers (step 2). Hence some residues between 1,444 and 1,481 are required for step 2.

Other residues between 1,274 and 1,467 (the last 30 nm of the coiled-coil) must also participate in step 2. First, the structure of the tetramers and the ability of C1,481 to form parallel dimers both indicate that the small domain between residues 1,444 and 1,481 must interact with the region around amino acid residue 1,360 of a parallel molecule (Fig. 1). Second, monoclonal antibodies that bind to sites centered at residues 1,460, 1,420, 1,400, and 1,390 can inhibit step 2 (Rimm et al., 1990).

Antiparallel interactions may also be involved in the second step, since two parallel dimers of C1,481 can associate in an antiparallel fashion to form a tetramer. The extensive antiparallel overlap in the center of the tetramers allows this to occur (Fig. 14 *b*). Since C1,481 forms parallel dimers with a 15-nm stagger, the tail piece is not essential for the parallel interactions. Native myosin-II does not form parallel dimers, because under conditions that promote the second step, the more favorable first step, formation of antiparallel dimers, has already gone to completion.

Step 3. Like the first two steps, a small region of the tail, in this case residues 1,410–1,430, is particularly important for the association of two tetramers to form octamers, but

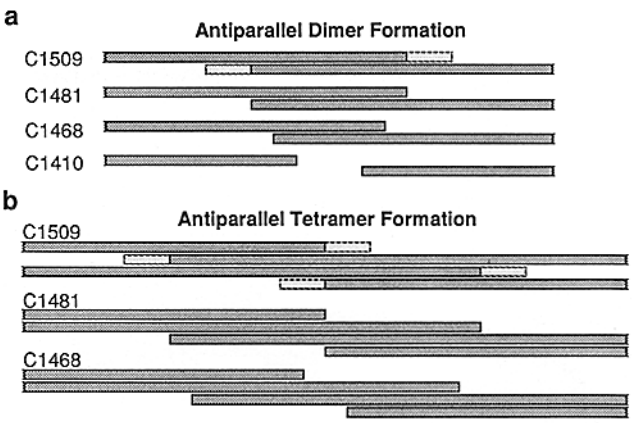

Figure 14. A diagrammatic representation of the fusion protein tails undergoing the first two steps in minifilament assembly. Fusion proteins containing deletions from the COOH terminus (tip of the tail) are shown in the orientation necessary to correctly assemble into a minifilament. Only the ends of the tails are shown. The lightly shaded region at the tips of the C1,509 tails represent the nonhelical tail piece. Molecular overlaps during (*a*) antiparallel dimer and (*b*) antiparallel tetramer formation are illustrated.

extensive contacts in the entire distal 30 nm of the tail also participate. Since the C1,443 fragment forms parallel dimers with a 30-nm stagger, residues 1410–1443 must interact with sequences 30 nm away near residue 1,225. Our experiments with monoclonal antibodies also implicate sites from 1,390 to 1,460 in the formation of octamers (Rimm et al., 1990).

Most of our work has emphasized the sequential nature of the three dimerization steps that lead to minifilaments, but the experiments with truncated molecules analyzed here and by others (Kuznicki et al., 1985; Hammer et al., 1987; Wijmenga et al., 1987), and the results with monoclonal antibodies (Rimm et al., 1990), illustrate that neither step 2 nor step 3 depends absolutely on the completion of the preceding steps. Nonetheless, the intermediates formed in steps 2 and 3 directly from monomers do not accumulate during the assembly of myosin-II, because the steps are progressively less favorable (Sinard and Pollard, 1990).

The Proximal Tail May Be Important for the Tight Packing of Molecules within the Minifilament

All the fusion proteins tested with intact COOH termini form octameric minifilaments with quantitatively normal properties and intermediates, but the presence or absence of the proximal part of the tail affects their structure after drying on mica. Native myosin and N881, which have the full length of the tail available for lateral associations, formed minifilaments that are more compact than N942 (Fig. 8), which lacks the first 6 nm of the tail or C1,509, which has this part of the tail obscured by trpE. These electron micrographs suggest that low affinity associations between the proximal parts of the tails play a role in stabilizing minifilaments, but we acknowledge that additional hydrodynamic studies will be required to confirm this hypothesis. The proposed interactions the proximal parts of the tails must involve molecules with 15-nm axial staggers since tetramers of myosin-II having only 15-nm staggers are tightly packed (Sinard et al., 1989).

Divalent Cation-induced Aggregation of Minifilaments Represents the Same Process as Paracrystal Formation

C1,509 minifilaments aggregate in divalent cations like myosin-II minifilaments, but the thick filaments of C1,509 have clearer striations than native myosin-II (Fig. 12 *c*). These striations are 15-nm apart and presumably represent the organized arrangement of the C1,509 heads. The C1,509 striations may be clearer, because the trpE head is attached more rigidly to the tail than the two myosin heads. The identical spacing of these axial striations and the head in minifilaments supports the theory that thick filaments are formed by the lateral aggregation of minifilaments and that the minifilaments are either in register or staggered axially by a multiple of 15 nm.

Under the same solution conditions, N942, which contains the same myosin tail sequence as C1,509 but lacks a head of any sort, forms much larger, paracrystalline structures with a ~15-nm pattern. Thus, the formation of paracrystals and thick filament are likely to be different manifestations of the same assembly process. The presence of the myosin or fusion protein heads apparently limits the extent of lateral aggregation, resulting in thick filaments. Since thick filaments are lateral aggregates of bipolar minifilaments, paracrystals may contain both parallel and antiparallel arrangements of myosin tails or tail fragments.

The regions of the myosin-II tail responsible for this higher order aggregation into thick filaments or paracrystals have not yet been well localized. C1,468 forms thick filaments, so the region of interest must be NH_2-terminal to residue 1,469. Molecules with larger deletions are not informative because they fail to form minifilaments, a prerequisite to thick filament formation (Sinard and Pollard, 1989). Point mutations or internal deletions rather than COOH-terminal deletions will be necessary to resolve this question.

Other Studies of Myosin Assembly Domains

The classic example of the localization of domains required for the assembly of myosin filaments is the proteolytic dissection of skeletal muscle myosin. Early studies showed that the distal two-thirds of the tail, called light meromyosin, is essential for assembly, while the proximal third of the tail, called subfragment-2, is soluble under physiological conditions (Lowey et al., 1969). More detailed studies on proteolytic fragments have localized residues important for assembly to a small region near the tip of the tail (Lu, R. C., L. Nyitray, M. Balint, and J. Gergeley. 1983. *Biophys. J.* 41 [No. 2, Pt. 2]: 288a [Abstr.]).

Analysis of fragments of the tail of *Dictyostelium* myosin-II produced in *E. coli* has been used to localize domains of *Dictyostelium* myosin-II required for paracrystal formation. A large fragment of the distal tail forms paracrystals in vitro (DeLozanne et al., 1987). Additional work with other clones further localized the assembly region to a 34-kD fragment ~34 kD in from the tip of the tail (O'Halloran et al., 1990). On the surface, this result suggests that there are fundamental differences in the assembly mechanisms of *Dictyostelium* and *Acanthamoeba* myosin-II, but the apparent differences may be related to the fact that the two studies have examined different assembly reactions. A firm conclusion must await a fuller characterization of the structure and the assembly mechanism of *Dictyostelium* myosin-II filaments.

We thank Carol Berkower of initial characterizations of C1,494 and C1,504, Craig Monell for help constructing the C1,328 clone, Donald Kaiser for preparing the monoclonal antibodies, and Pam Maupin for her assistance in preparing the samples for electron microscopy.

This work was funded by Medical Scientist Training Program awards to J. H. Sinard and D. L. Rimm (GM-07309) and a National Institutes of Health research grant to T. D. Pollard (GM-26132).

Received for publication 18 June 1990 and in revised form 29 August 1990.

References

Cohen, C., S. Lowey, R. G. Harrison, J. Kendrick-Jones, and A. G. Szent-Gyorgyi. 1970. Segments from myosin rods. *J. Mol. Biol.* 47:605–609.

Coté, G. P., E. A. Robinson, E. Apella, and E. D. Korn. 1984. Amino acid sequence of a segment of the *Acanthamoeba* myosin-II heavy chain containing all three regulatory phosphorylation sites. *J. Biol. Chem.* 259:12781–12787.

Davis, J. S. 1988. Asssembly processes in vertebrate skeletal thick filament formation. *Annu. Rev. Biophys. Biophys. Chem.* 17:217–239.

DeLozanne, A., C. H. Berlot, L. A. Leinwand, and J. A. Spudich. 1987. Expression in *Escherichia coli* of a functional *Dictyostelium* myosin tail fragment. *J. Cell Biol.* 105:2999–3005.

Hammer, J. A., B. Bowers, B. M. Patterson, and E. D. Korn. 1987. Complete nucleotide sequence and deduced polypeptide sequence of a nonmuscle myosin heavy chain gene from *Acanthamoeba*: evidence of a hinge in the rodlike tail. *J. Cell Biol.* 105:913–925.

Huxley, H. E., and W. Brown. 1967. The low-angle x-ray diagram of vertebrate striated muscle and its behavior during contraction and rigor. *J. Mol. Biol.* 30:383–434.

Kuznicki, J., G. P. Cote, B. Bowers, and E. D. Korn. 1985. Filament formation and actin-activated ATPase activity are abolished by proteolytic removal of a small peptide from the tip of the tail of the heavy chain of *Acanthamoeba* myosin-II. *J. Biol. Chem.* 260:1967–1972.

Lowey, S., H. S. Slayter, A. G. Weeds, and H. Baker. 1969. Substructure of the myosin molecule I. Subfragments of myosin produced by enzymatic digestion. *J. Mol. Biol.* 42:1–29.

Maniatis, T., E. F. Fritsch, and J. Sambrook. 1982. Molecular Cloning. A Laboratory Manual. Cold Spring Harbor Laboratory, Cold Spring Harbor, NY. 545 pp.

Mejbaum-Katzenellenbogen, W., and W. M. Dobryszycka. 1959. New method for quantitative determination of serum proteins separated by paper electrophoresis. *Clin. Chim. Acta.* 4:515–522.

O'Halloran, T. J., S. Ravid, and J. A. Spudich. 1990. Expression of *Dictyostelium* myosin tail segments in *Escherichia coli*: domains required for assembly and phosphorylation of *E. coli* expressed. *J. Cell Biol.* 110:63–70.

Pollard, T. D. 1982. Structure and polymerization of *Acanthamoeba* myosin-II filaments. *J. Cell Biol.* 95:816–825.

Pollard, T. D., W. F. Stafford, and M. E. Porter. 1978. Characterization of a second myosin from Acanthamoeba castellanii. *J. Biol. Chem.* 253:4798–4808.

Reisler, E., C. Smith, and G. Seegan. 1980. Myosin minifilaments. *J. Mol. Biol.* 143:129–145.

Rimm, D. L., and T. D. Pollard. 1989. New plasmid vectors for high level synthesis of eukaryotic fusion proteins in *Escherichia coli*. *Gene (Amst.).* 75:323–327.

Rimm, D. L., J. H. Sinard, and T. D. Pollard. 1989. Location of the head-tail junction of myosin. *J. Cell Biol.* 108:1783–1789.

Rimm, D. L., D. A. Kaiser, D. Bhandari, P. Maupin, D. P. Kiehart, and T. D. Pollard. 1990. Identification of functional regions on the tail of *Acanthamoeba* myosin-II using recombinant fusion proteins. I. High resolution epitope mapping and characterization of monoclonal antibody binding sites. *J. Cell Biol.* 111:2405–2416.

Sinard, J. H., and T. D. Pollard. 1989. The effect of phosphorylation and solution conditions on the steady-state assembly of *Acanthamoeba* myosin-II. *J. Cell Biol.* 107:1529–1535.

Sinard, J. H., and T. D. Pollard. 1990. *Acanthamoeba* myosin-II minifilaments assemble on a millisecond time scale with rate constants greater than those expected for a diffusion limited reaction. *J. Biol. Chem.* 265:3654–3660.

Sinard, J. H., W. F. Stafford, and T. D. Pollard. 1989. The mechanism of assembly of *Acanthamoeba* myosin-II minifilaments: minifilaments assemble by three successive dimerization steps. *J. Cell Biol.* 107:1537–1547.

Trybus, K. M., and S. Lowey. 1987. Assembly of smooth muscle myosin minifilaments: effects of phosphorylation and nucleotide binding. *J. Cell Biol.* 105:3007–3019.

Wijmenga, S. S., M. A. L. Atkinson, D. Ray, and E. D. Korn. 1987. Electric birefringence study of the solution structure of chymotrypsin-cleaved *Acanthamoeba* myosin-II. *J. Biol. Chem.* 262:15803–15808.